Geog0067 Surface Water Modelling Coursework

Content

Part 1 Implementation of a Telemac 2D storm surge inundation model for the Port of Immingham

Introduction

Storm surge inundation is a serious coastal hazard that can have catastrophic effects on people, property, and the ecosystem. Strong winds, low atmospheric pressure, and high tides come together to generate a considerable rise in water levels along the shore, which causes floods and harm to coastal areas (Needham, Keim and Sathiaraj, 2015). The frequency and intensity of storm surges are anticipated to grow as global climate change continues to have an impact on weather patterns, escalating the dangers faced by coastal communities around the world (IPCC, 2019).

This growing concern extends to the Port of Immingham in the UK, which is situated on the Humber Estuary. Due to its importance as a port for both domestic and international trade, the area's economy, infrastructure, and local populations are significantly at risk from storm surge inundation (Environment Agency, 2008; Wadey *et al.*, 2015). Storm surge events are more likely to have serious repercussions due to the Humber Estuary's particular geography, which comprises a wide and shallow estuary and tidal influences (Brown, Souza and Wolf, 2010). Additionally, because of its location in a low-lying area, the Port of Immingham is quite vulnerable to flooding from storm surges (Horsburgh and Wilson, 2007).

Figure 1. Site location

In this report, a mesh for the research region will first be generated using the BlueKenue software, which will provide a thorough depiction of the Port of Immingham's coastline and bathymetric features. After that, a Telemac 2D storm surge inundation model will be used to simulate and examine the effects of storm surges on the port. This report aims to thoroughly understand storm surge inundation modelling and give some insights for future decision-making about flood risk management and mitigation tactics.

Model implementation

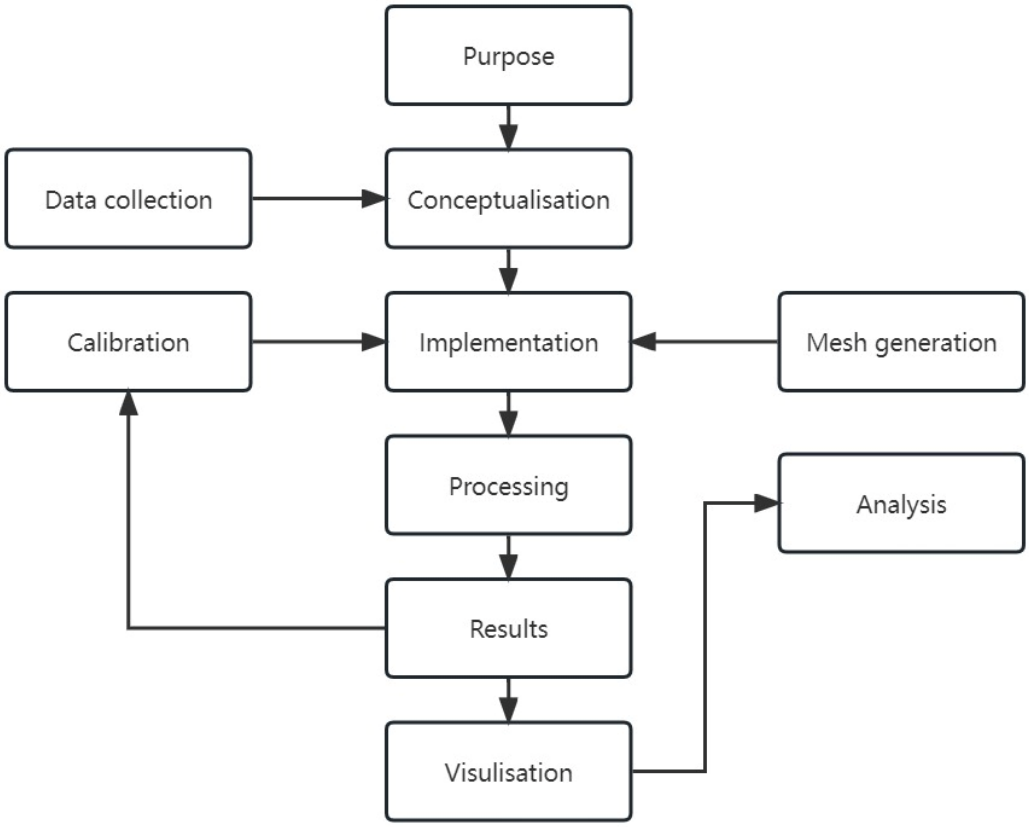

Figure 2. Workflow of modelling

Model type

A numerical finite volume scheme was used to develop the implemented model, which was created specifically for emulating hydrodynamic processes in coastal and estuarine environments. The model is built upon the Telemac 2D framework, which solves the Saint-Venant equations by using a depth-averaged shallow water technique while taking into consideration the conservation of mass and momentum(Hervouet, 2007).

Computer implementation

The Telemac 2D software package was run on a Linux-based system to implement the model. The programme in Telemac 2D was created in Fortran 95 and was built with Intel compilers connected to MPI libraries. This makes it possible to divide the calculation among several CPU cores, improving efficiency and slashing the time needed for model runs.

Domain discretization and mesh generation

The T3 Mesh Generator in the Blue Kenue programme was utilised for the domain discretization and mesh generation (National Research Council Canada, 2019). A lot of mesh configurations were investigated, including the insertion of density points, hard lines, and soft lines. Furthermore, the T3 Channel Mesher was also utilised to generate a sub-mesh for the dock entrance area, where a finer mesh resolution was needed due to high flow rates and probable numerical stability problems.

Parameters and boundary conditions

To precisely define the hydrodynamic processes in the study area, parameters and boundary conditions were determined as follows. Firstly, a Selafin file was used to incorporate the model's bathymetry data into the mesh. Then, the boundary conditions were stored in a separate text file. The model utilised a Thompson Boundary Condition for the landward boundary and took into consideration an imposed sea level (H) at the offshore boundary. Additionally, a steering file that integrates all information needed to run the model is used to control the input parameters and model settings, enabling convenient adjustment between runs.

Model runs

To assess the hydrodynamic model's performance and sensitivity under various scenarios, four model experiments were conducted in this study. The first experiment compared the maximum flood depth with the observed flood extent polygon using the F statistic to examine the sensitivity of the modelled flood extent to various friction coefficients. Then, the optimal friction coefficient was adopted in the following experiments. In the second experiment, the accuracy of the high-resolution hydrodynamic flood inundation model was compared to that of a less complicated GIS-based static inundation method. The third experiment changed the number of CPU cores being used to examine the effect of parallel computing on model run time. Finally, the fourth experiment explored the impact of sea-level rise on inundation extent for a 1:750-year event, using two future scenarios with differing peak water levels (5.55 m ODN and 6.0 m ODN) to grasp the potential increase in flood extent due to sea-level rise.

Results and analysis

Experiment 1

Table 1. F statistic for runs with different friction coefficient

Friction coefficient	0.1	0.2	0.3	0.4	0.5	0.35
F statistic	0.44645	0.51561	0.61553	0.60394	0.55999	0.61747

Obviously, when friction coefficient was 0.35, F statistic was highest. Below were the outputs for this run.

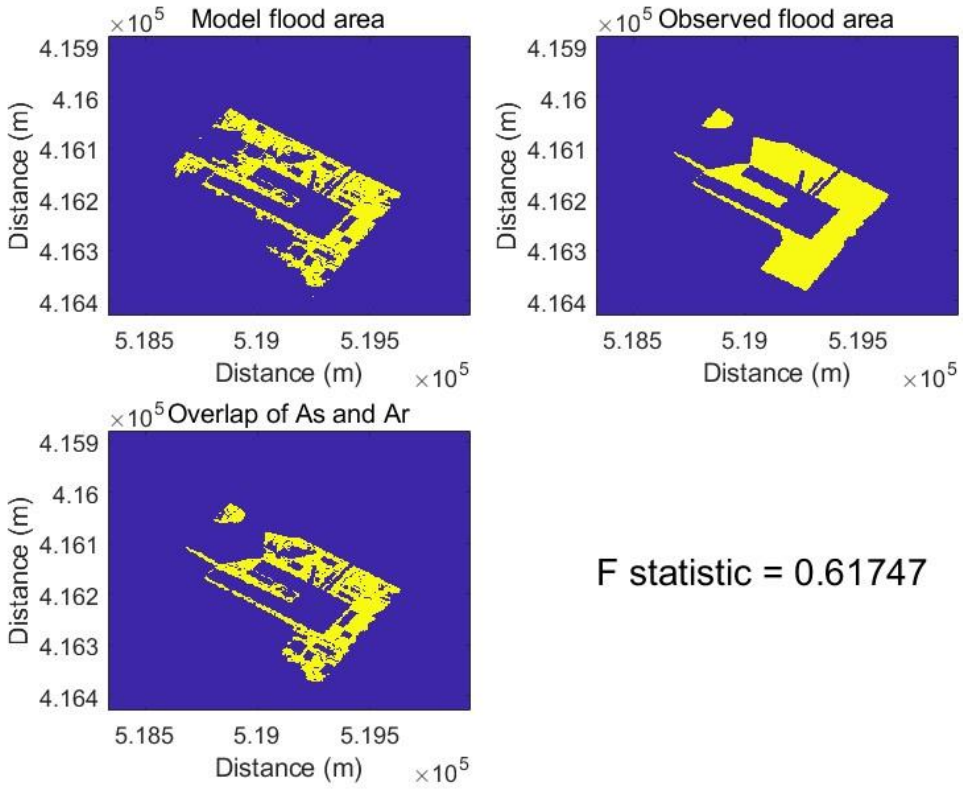

Figure 2. Best performed model output

Experiment 2

The graphs below compared result generated by GIS-based static inundation method with the best performing model from Experiment 1. Here, the black line closed area represented the observed flood extent.

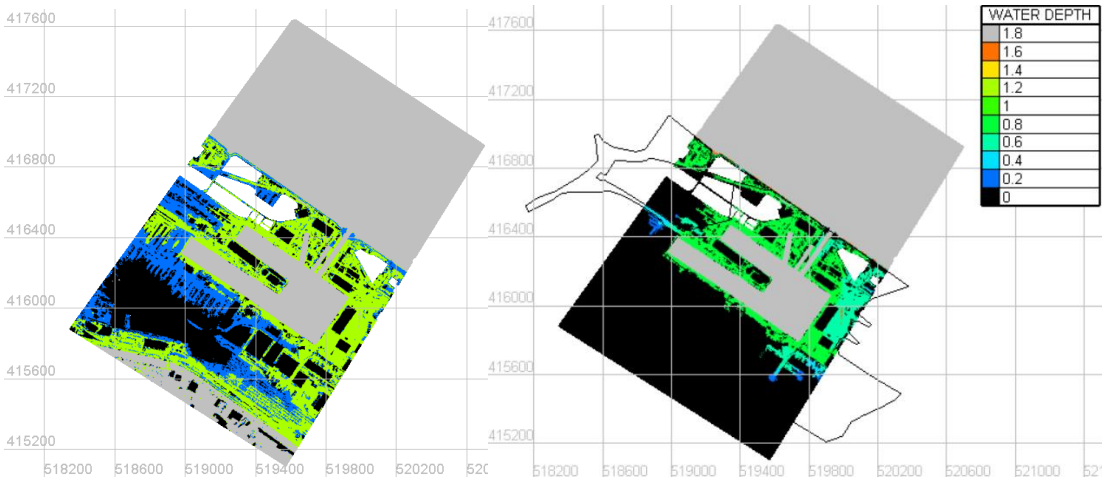

(a)GIS-based static inundation method model (b)Telemac2D simulated model

Figure 3. Comparison of modelled flood extent with GIS-based static inundation method

Obviously, the performance of GIS-based static inundation method was terrible. Its flood extent significantly exceeds the observed extent, compared to the Telemac2D simulated model.

Experiment 3

Table 2. Model run time with different ncsize

ncsize	1	2	3	4	8
Time	30m59s	19m44s	17m01s	15m44s	14m51s

Here, ncsize means the number of CPU cores being used in model running. The relationship between ncsize and time can be visualized in the figure below:

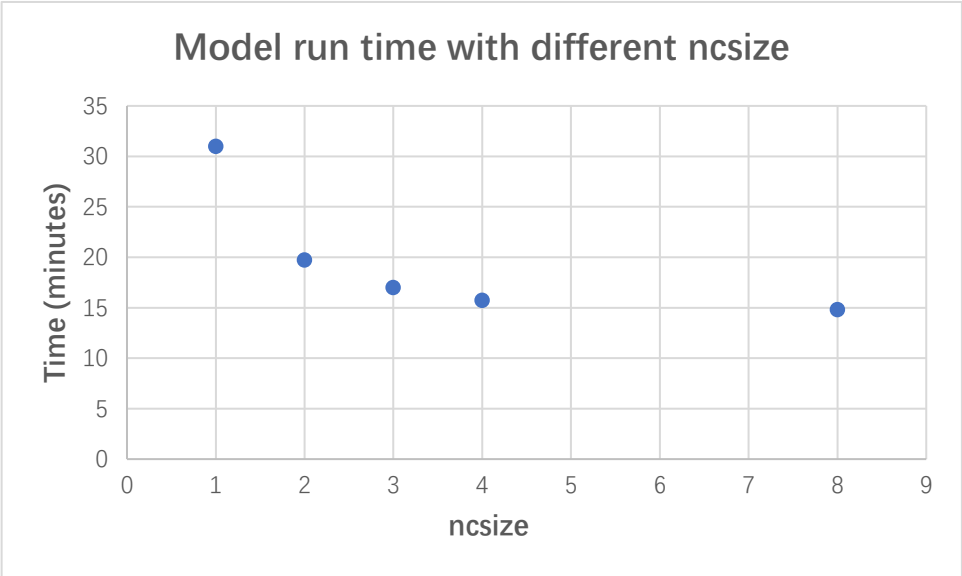

Figure 4. Model run time with different number of computing cores applied

As shown in **Figure 4.**, the model run time dramatically decreased when ncsize was increased from 1 to 2. The running speed kept increasing when more CPU cores were adopted, but the growth rate gradually slowed down. From ncsize=4 to 8, the improvement was no longer significant.

Experiment 4

The following graphs visualized the model results under different tidal surge time series, which were 2013 scenario, 2065 scenario, and 2115 scenario, respectively. Here, the black line closed area represented the observed flood extent for reference.

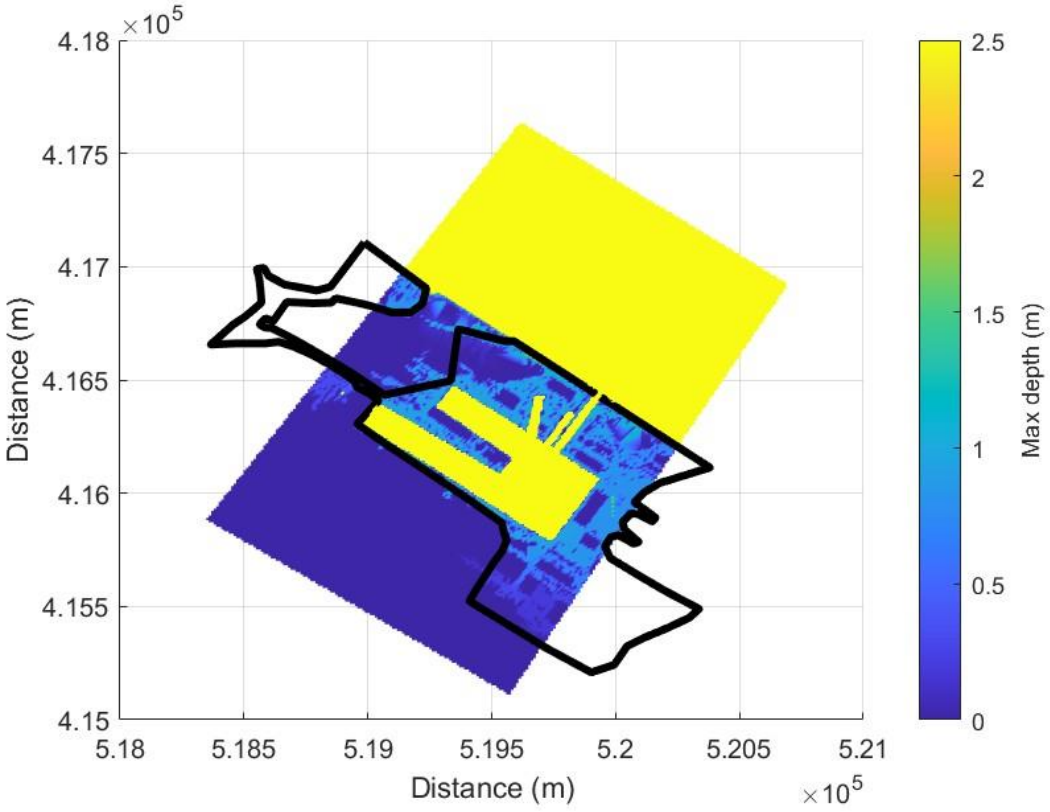

(a)Flooding under a 1:750 surge event in 2013

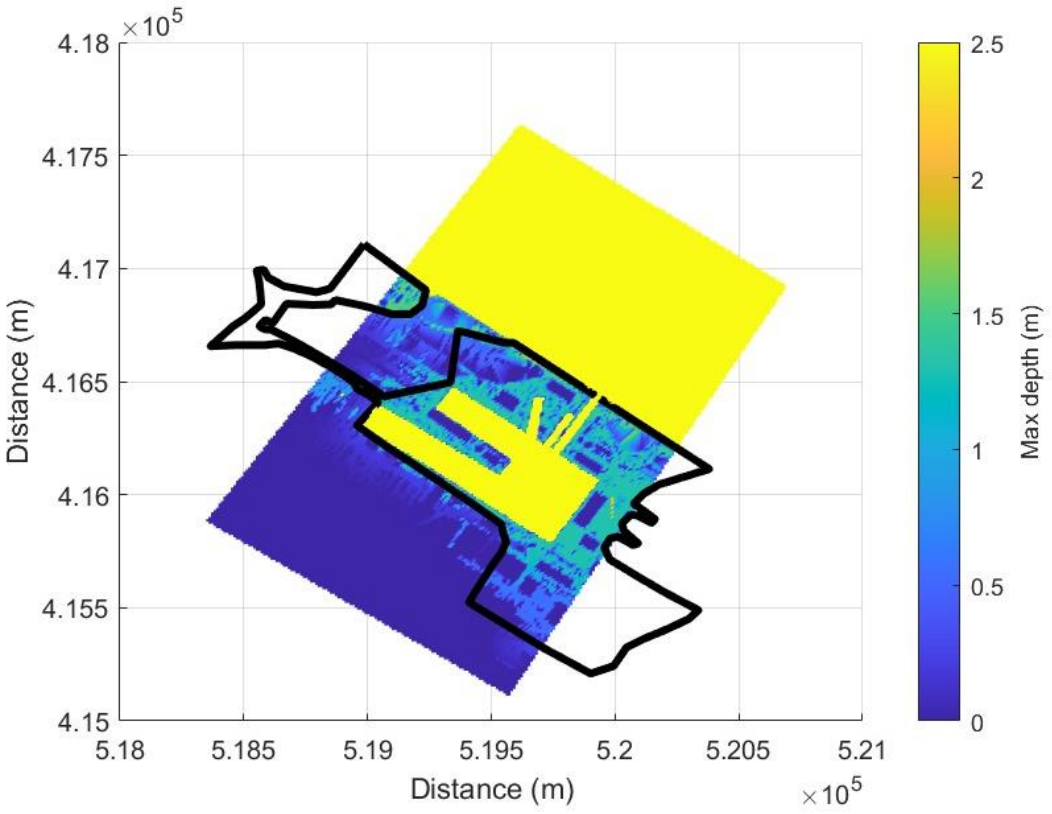

(b)Flooding under a 1:750 surge event in 2065

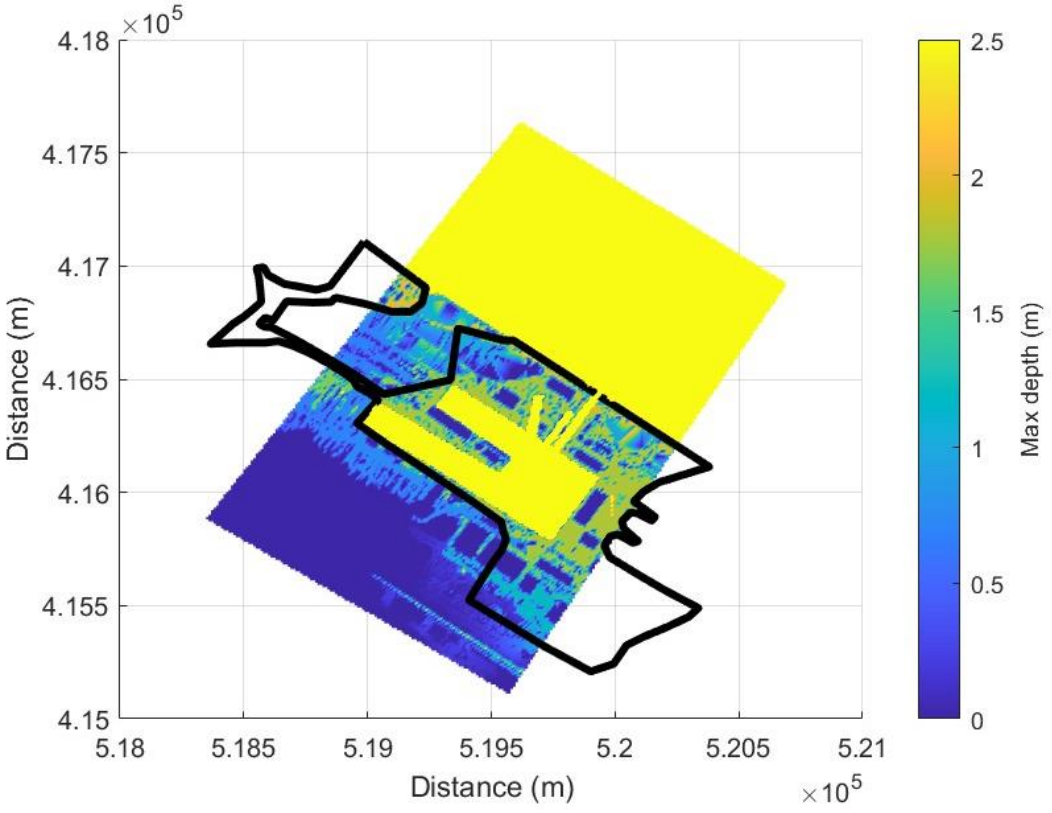

(c)Flooding under a 1:750 surge event in 2115

Figure 5. Model results' visualization under different tidal surge time series

Comparing the three graphs it could be concluded that the max depth on the flood region increased with the sea-level rise. The increase from 2013 to 2065 and then to 2115 is approximately 0.5 meters for each. Additionally, the flooding area expanded outward correspondingly.

Discussion and conclusions

The results of the experiments conducted in this study offered important understandings of the functionality of the Telemac 2D storm surge inundation model and its relevance to the Port of Immingham.

Experiment 1's sensitivity analysis showed how crucial it is to choose the right friction coefficient, with a value of 0.35 producing the highest F statistic. This result was in line with earlier research (Pappenberger *et al.,* 2005).

Experiment 2 demonstrated the limitations of the GIS-based static inundation method, with its flood extent greatly exceeding the observed extent when compared to the more accurate Telemac 2D simulated model. This highlighted the importance of using advanced hydrodynamic models such as Telemac 2D to better understand and anticipate the effects of storm surge inundation.

Experiment 3 results highlighted the efficiency advantages realised by parallel computing in lowering model run times. Although the improvement in run times decreased as the number of CPU cores increased, the overall time reduction was still significant and useful for model applications.

Finally, Experiment 4 showed how sea-level rise could affect the amount and depth of flooding in the Port of Immingham during a 1:750-year storm surge event. The model results showed a 0.5meters rise in maximum flood depth for each scenario (2013, 2065, and 2115), as well as a commensurate expansion in the inundated region. This data was critical for decision-makers and stakeholders devising effective flood risk management strategies and adaptation measures in response to the expected impacts of climate change (Nicholls *et al.,* 2011).

In conclusion, this study stated the importance of the Telemac 2D storm surge inundation model for the Port of Immingham and provided insight into the potential implications of sea-level rise on the area. The findings emphasised the importance of employing advanced hydrodynamic models and parallel computing technologies when modelling storm surge flooding. These findings could have an impact on future research and decision-making in the context of coastal flood risk management and adaptation planning.

Part 2 MIKE-SHE distributed hydrological model

Introduction

Climate change could extensively impact river systems. Specifically, surface runoff, infiltration, and evapotranspiration may result from changing precipitation patterns and more frequent extreme events as global temperatures rise (Bates *et al.*, 2008). To develop efficient mitigation and adaptation strategies, it is essential to understand these potential effects. The Karup catchment in Denmark, functions as a crucial water resource for human consumption and environmental health, is one location of particular importance. The catchment is distinguished by varied land use, various hydrogeological settings, sandy and clayey soils, and shallow and deep aquifers, making it a valuable case study for exploring the potential implications of climate change on hydrological systems.
Several experiments were carried out, including the creation of a catchment model using MIKE SHE and its connection with a river model created using the 1-D hydraulic model MIKE 11. The model was calibrated and validated after the development process was finished. Following that, an opportunity would be given to investigate various climate change-related scenarios. This study aimed to develop adequate skill in utilising the cutting-edge model MIKE-SHE, which would aid in gaining useful insights into the potential implications of climate change on catchment hydrology(Refsgaard *et al.*, 2013).

Model implementation

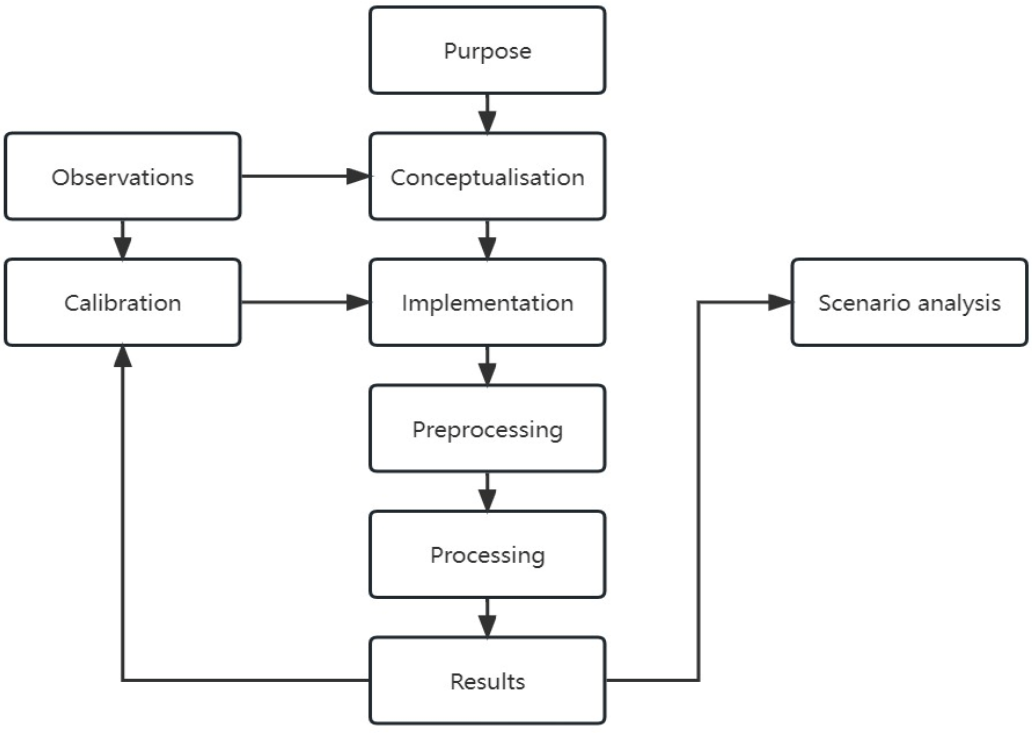

Figure 6. Workflow of modelling

Model type

A numerical finite element scheme was employed in this study, using the MIKE-SHE model developed by DHI for simulating hydrological processes (Abbott *et al.*, 1986). The model, which accounts for key hydrological processes such as overland flow, unsaturated zone flow, groundwater flow, and river flow, is a physically based, distributed, and deterministic tool (Graham and Butts, 2005).

Computer implementation

The MIKE SHE model was implemented using the MIKE Zero software package, executed on a standard computer with a Windows operating system.

Domain discretization and mesh generation

The domain discretization and mesh generation were carried out with the help of the MIKE Zero Grid Editor, which allows for the design and editing of computational grids for the model. A regular grid with a specific cell size was used to cover the Karup catchment region.

Parameters and boundary conditions

Parameters and boundary conditions were specified to appropriately depict the hydrological processes in the Karup catchment. These included the sand aquifer and clay lenses' horizontal and vertical hydraulic conductivity, meteorological inputs like precipitation and potential evapotranspiration, observations of the river network and discharge, and the distribution of vegetation and different land cover types (Thompson *et al.*, 2014).

Model runs

Calibration and validation of the model were completed before an analysis of the effects of climate change. Key parameters were iteratively changed to minimise disparities between simulated and observed river discharge and groundwater levels. A split-sample methodology was used for calibration and validation, and statistical measures were used to assess model performance. After being validated, the model was used to evaluate the effects of climate change on the catchment using perturbed meteorological inputs, such as daily precipitation and potential evapotranspiration (PET), based on low, medium, and high emissions scenarios for the year 2050. Then, analysis was done on how these new data affected groundwater levels and river discharge, as well as how sensitive the catchment was to variations in precipitation and PET.

Results and analysis

The following figures were all generated by python, the coded were uploaded on: https://github.com/ucfaune/GEOG0067-Surface-Water-Modelling/blob/main

Calibration

After substituting several different sets of calibration parameters within the potential range, the parameters were set as **Table 3.**. Here, only the change on Horizontal Hydraulic Conductivity of Sand Aquifer could lead to significant difference on model performance, so other three parameters were all taken as the middle value of the suggested range.

Table 3. Best group of parameters

Horizontal Hydraulic Conductivity		Vertical Hydraulic Conductivity	
Sand Aquifer	Clay Lenses	Sand Aquifer	Clay Lenses
3.9E-04	5E-06	5E-05	5E-05

The model outputs under this group of parameters were separately plotted as follow:

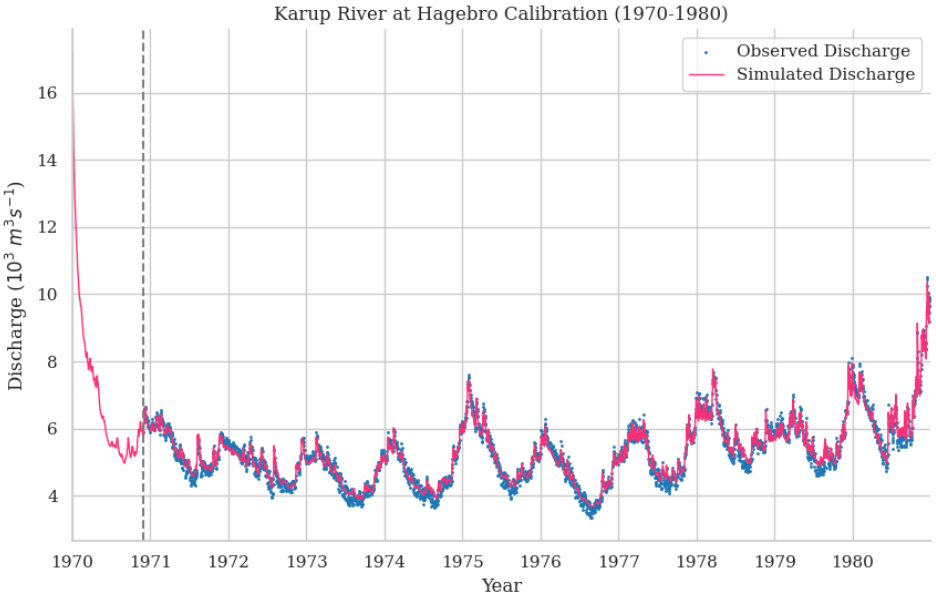

(a)Simulation compared with observation at Hagebro

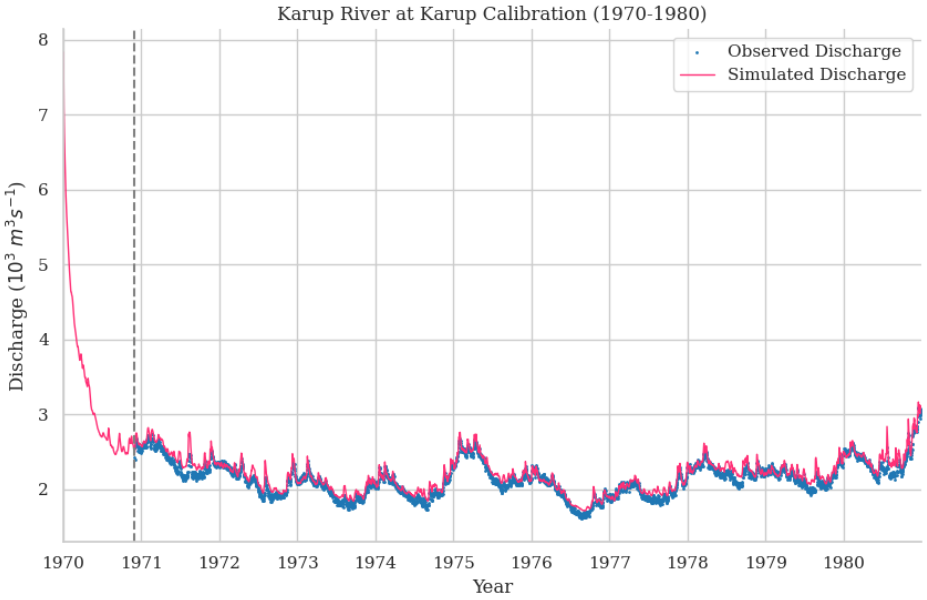

(b)Simulation compared with observation at Karup

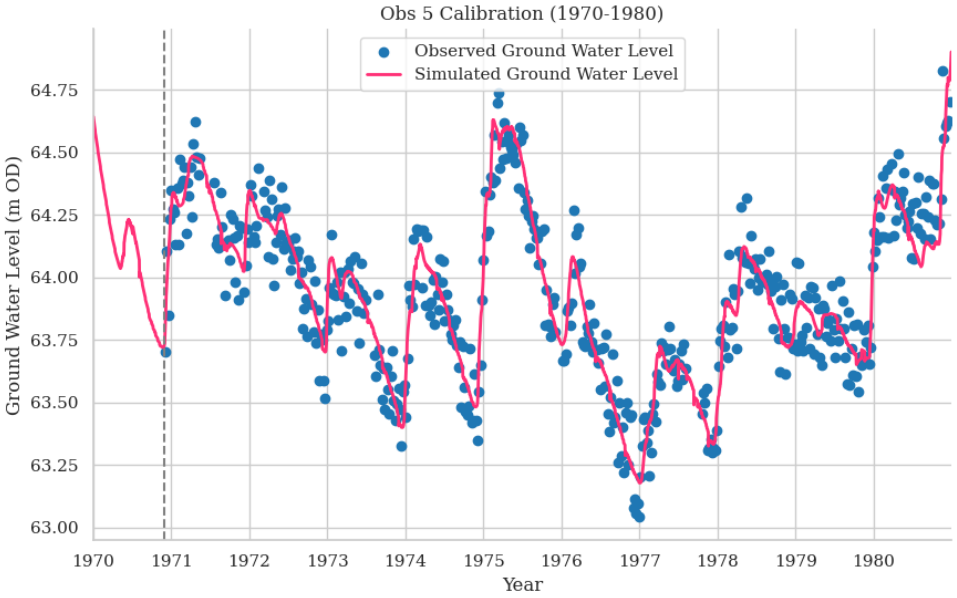

(c)Simulation compared with observation at Obs 5

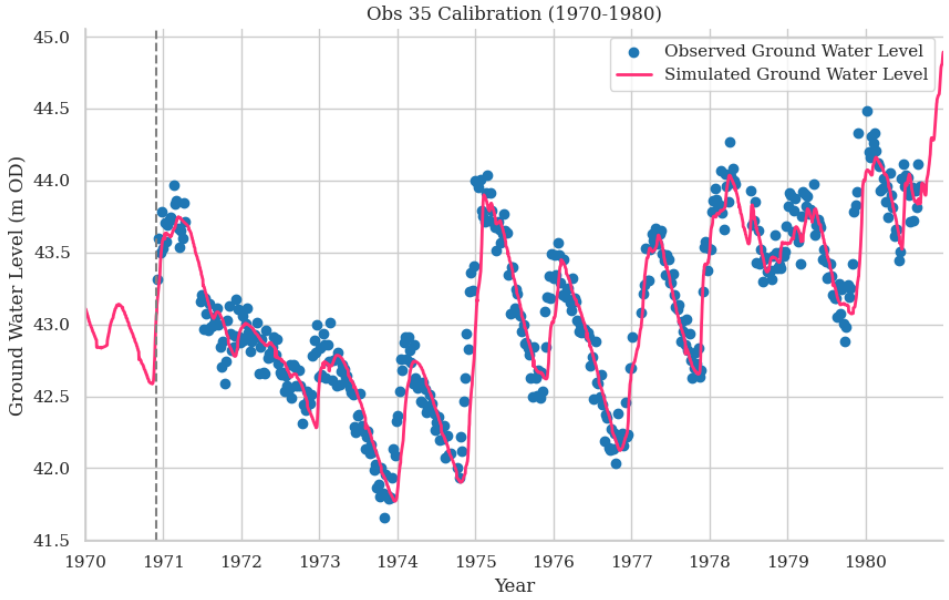

(d)Simulation compared with observation at Obs 35

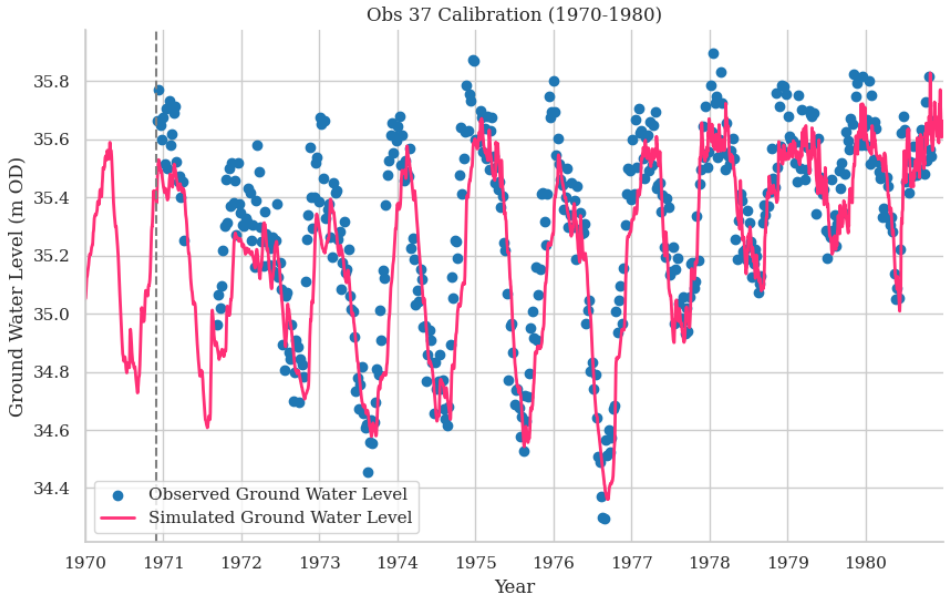

(e)Simulation compared with observation at Obs 37

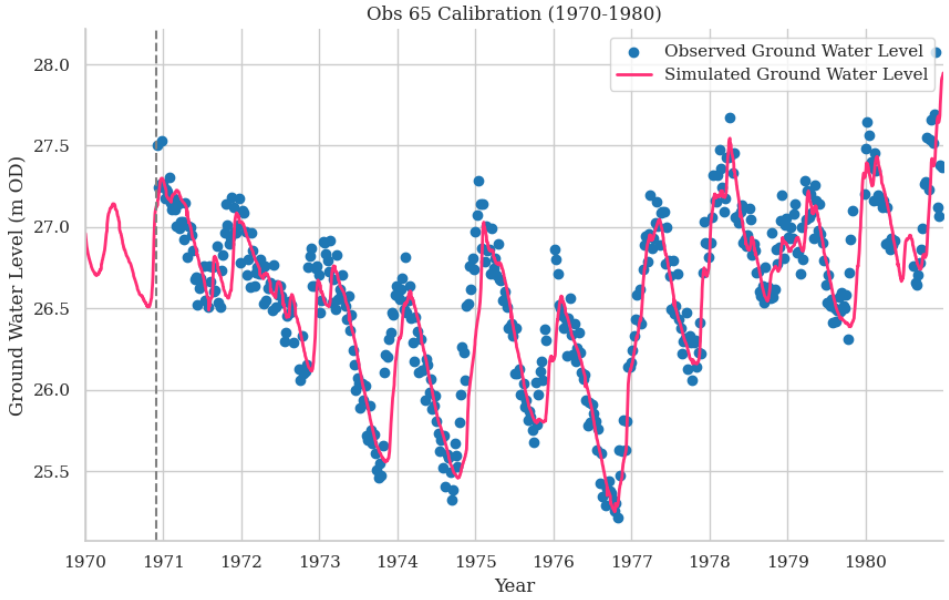

(f)Simulation compared with observation at Obs 37

Figure 7. Calibration results with best parameters

As shown in the **Figure 7.**, the simulated trend line for all stations approximately matched with the corresponding observed data. Especially, the observation and the simulation related to river discharge had a high degree of consistency. The same result could also be obtained by statistical assessment in Table below, where Dv was percentage deviation in simulation from the observation, NSE was Nash-Sutcliffe coefficient and r was correlation coefficient (Henriksen *et al.*, 2008).

Table 4. Statistical assessment for calibrated result

Station	Period	Dv (%)		NSE		r
Obs 5	1970.12.01-1980.12.31	+0.01	N/A	0.886	N/A	0.942
Obs 35	1970.12.01-1980.12.31	-0.08	N/A	0.861	N/A	0.930
Obs 37	1970.12.01-1980.12.31	-0.23	N/A	0.675	N/A	0.862
Obs 65	1970.12.01-1980.12.31	-0.16	N/A	0.810	N/A	0.908
Karup River at Hagebro	1970.12.01-1980.12.31	+0.22	☆☆☆☆☆	0.974	☆☆☆☆☆	0.988
Karup River at Karup	1970.12.01-1980.12.31	+2.70	☆☆☆☆☆	0.882	☆☆☆☆☆	0.972

Performance indicator	Excellent	Very good	Fair	Poor	Very poor
	☆ ☆ ☆ ☆ ☆	☆ ☆ ☆ ☆	☆ ☆ ☆	☆ ☆	☆
Dv	<5%	5-10%	10-20%	20-40%	>40%
NSE	>0.85	0.65-0.85	0.50-0.65	0.20-0.50	<0.20

Investigation of climate change

The following figures shown the model output from only precipitation modified and only PET modified, to study which one had more impact on the model result.

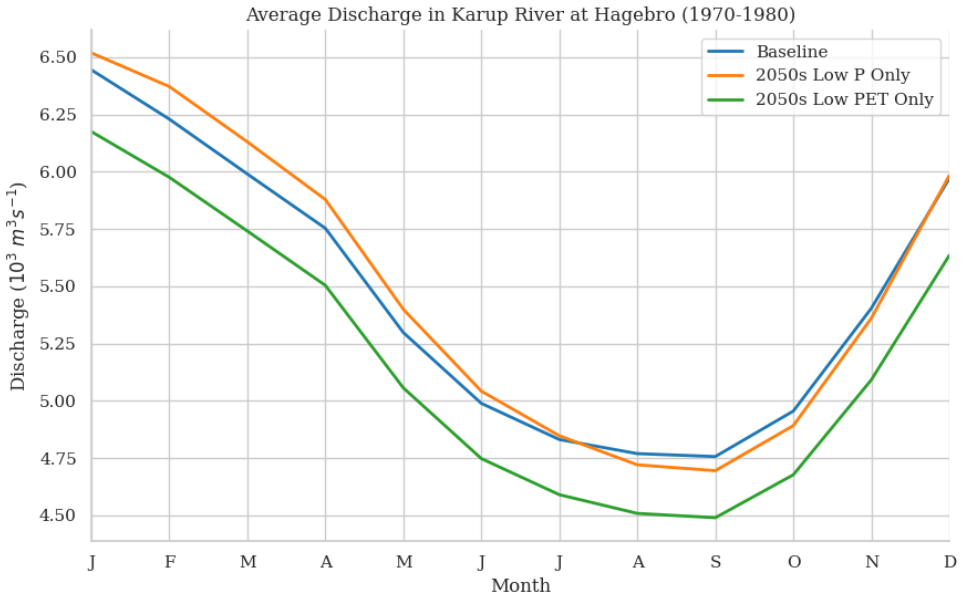

(a)Discharge at Hagebro

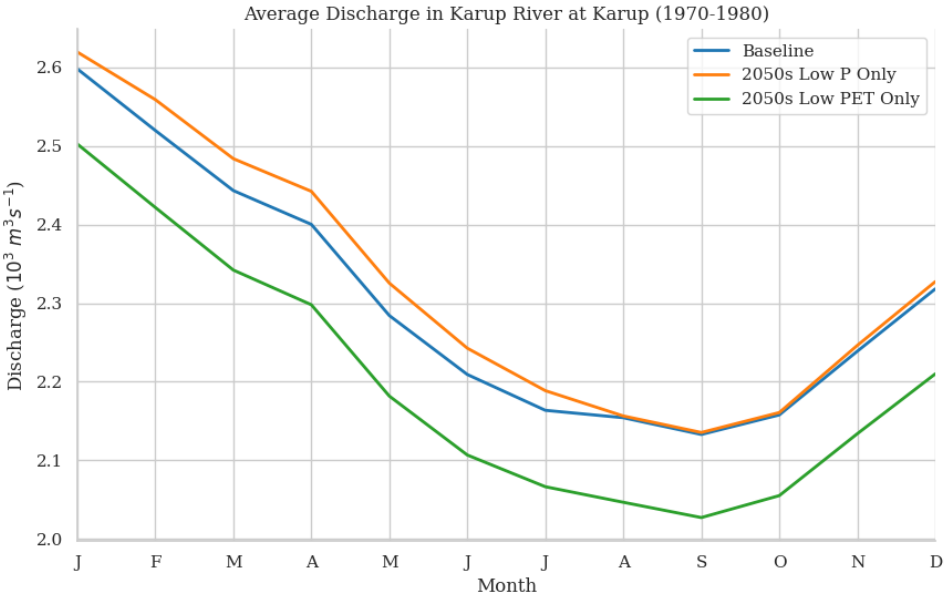

(b)Discharge at Karup

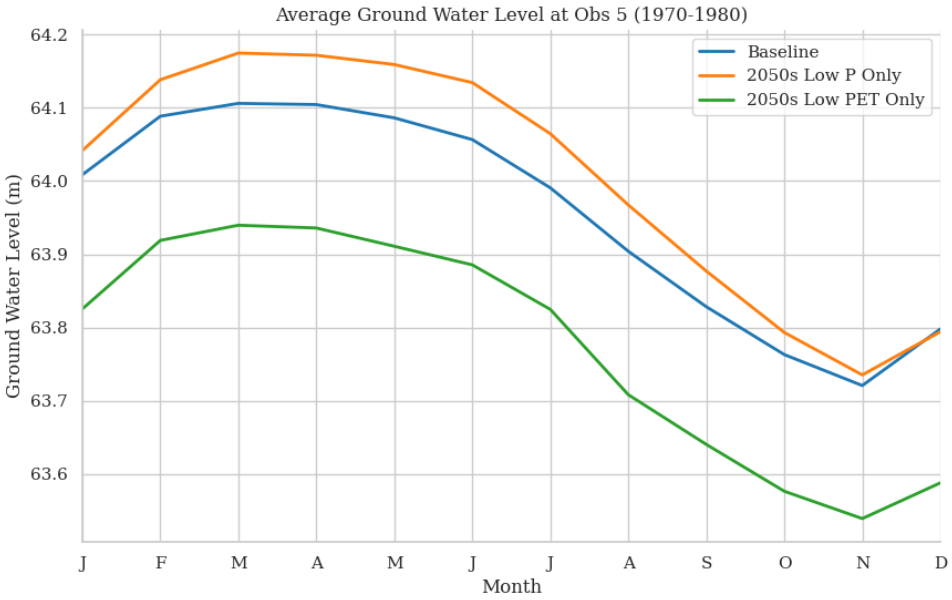

(c)Ground water level at Obs 5

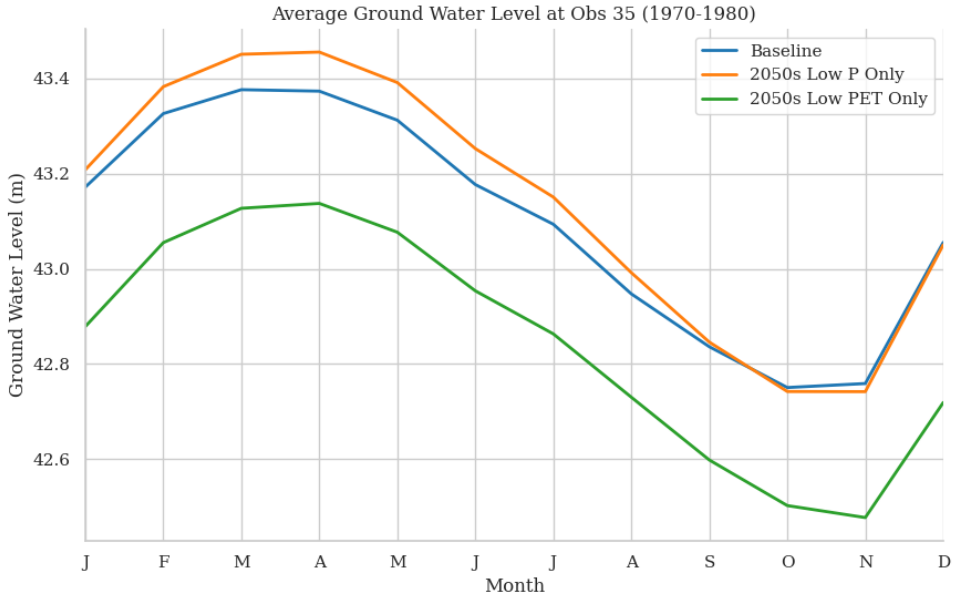

(d)Ground water level at Obs 35

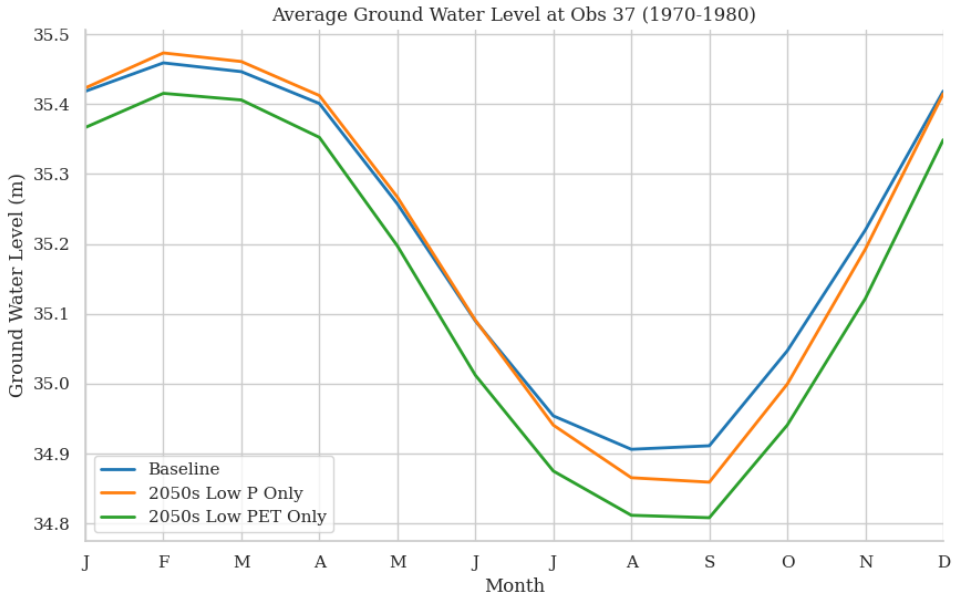

(e)Ground water level at Obs 37

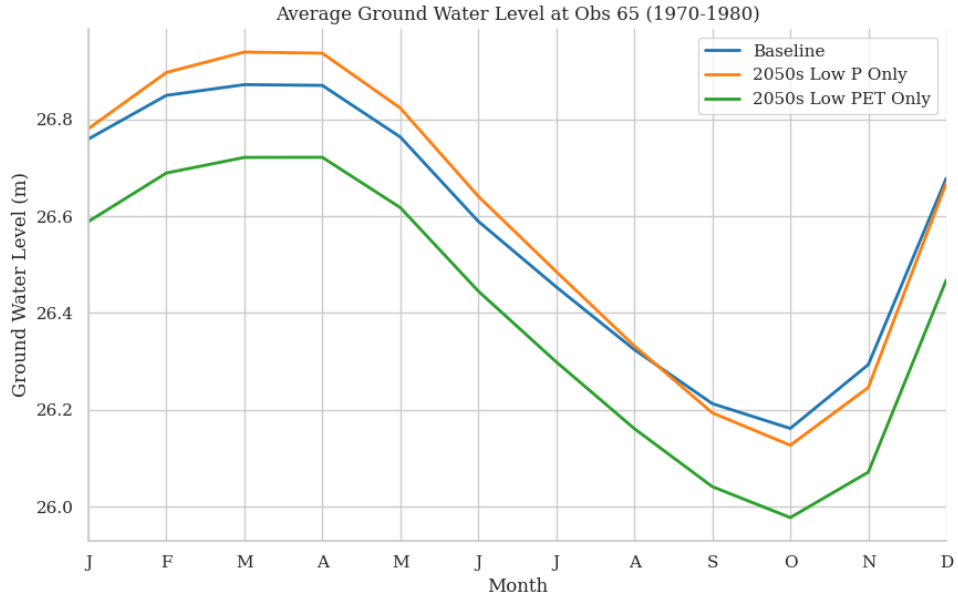

(f)Ground water level at Obs 65

Figure 8. The output results of model under only P modified and only PET modified scenarios

Obviously, the model results were more sensitive to the change of PET which led to a significant difference from the baseline.

The following figures presented the results of the model run under three different scenarios: Low Emissions Scenario projected to the 2050s, Medium Emissions Scenario projected to the 2050s, and High Emissions Scenario projected to the 2050s. In the figures, the data for each month represented the average value of all daily data within that month over the 1970-1980 period.

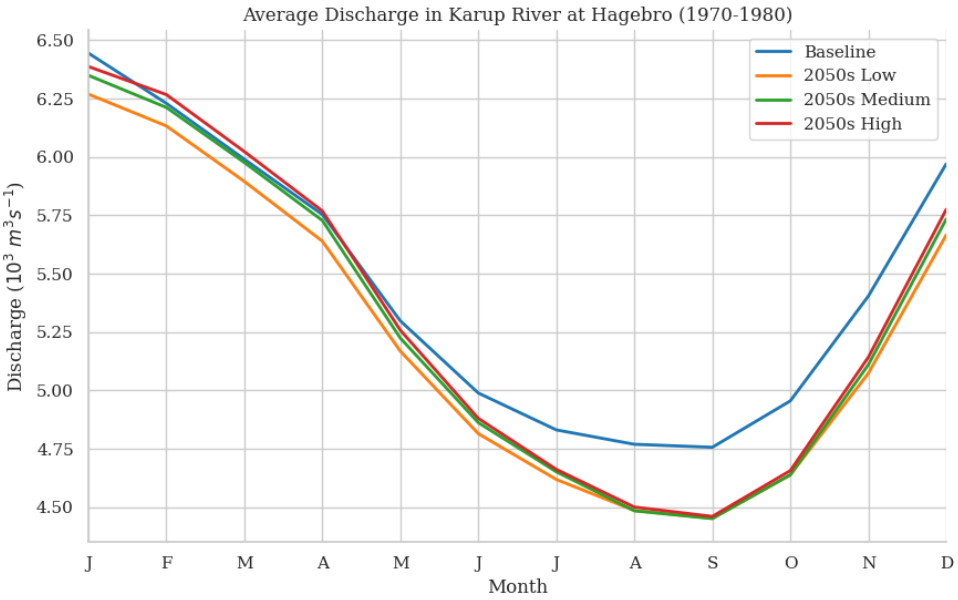

(a)Discharge at Hagebro

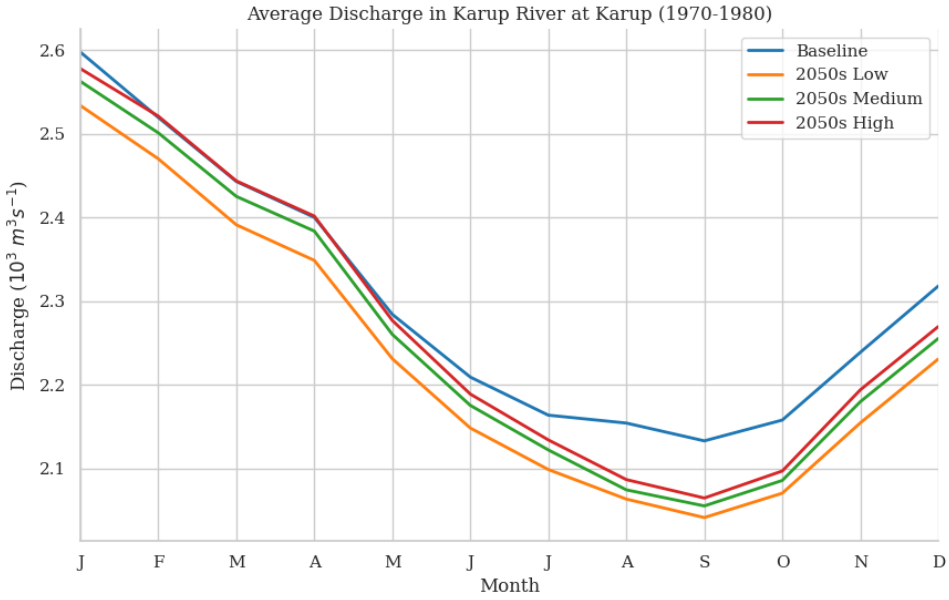

(b)Discharge at Karup

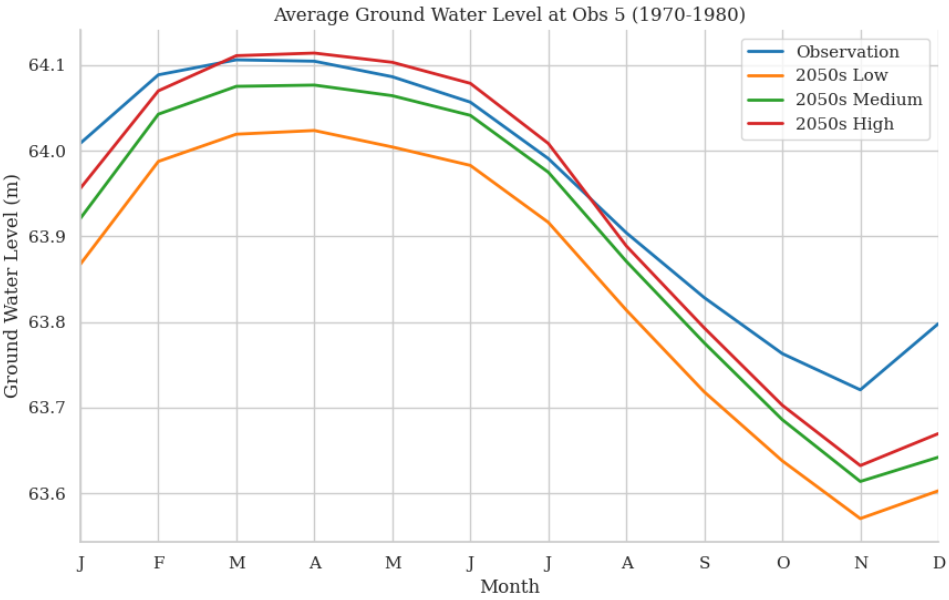

(c)Ground water level at Obs 5

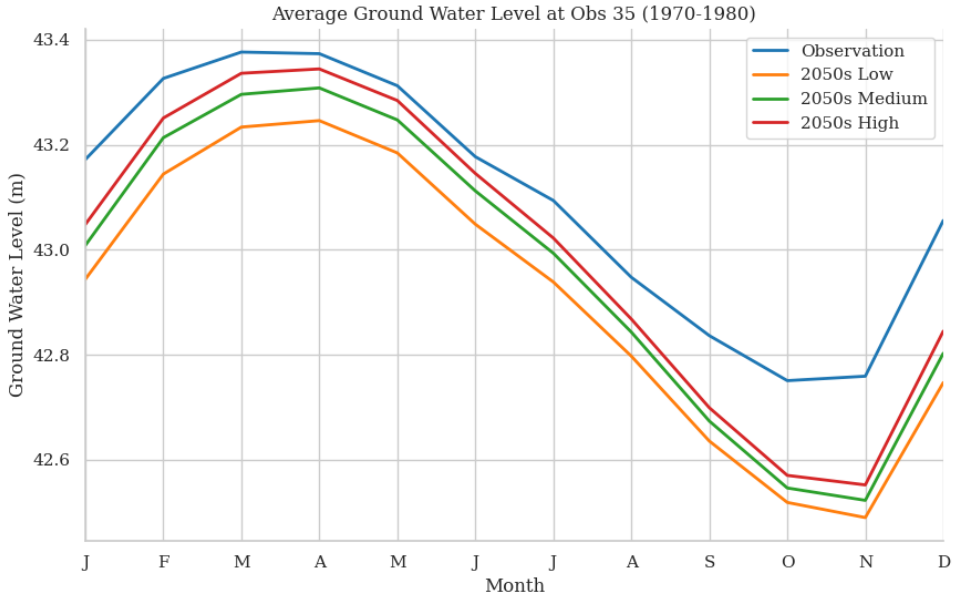

(d)Ground water level at Obs 35

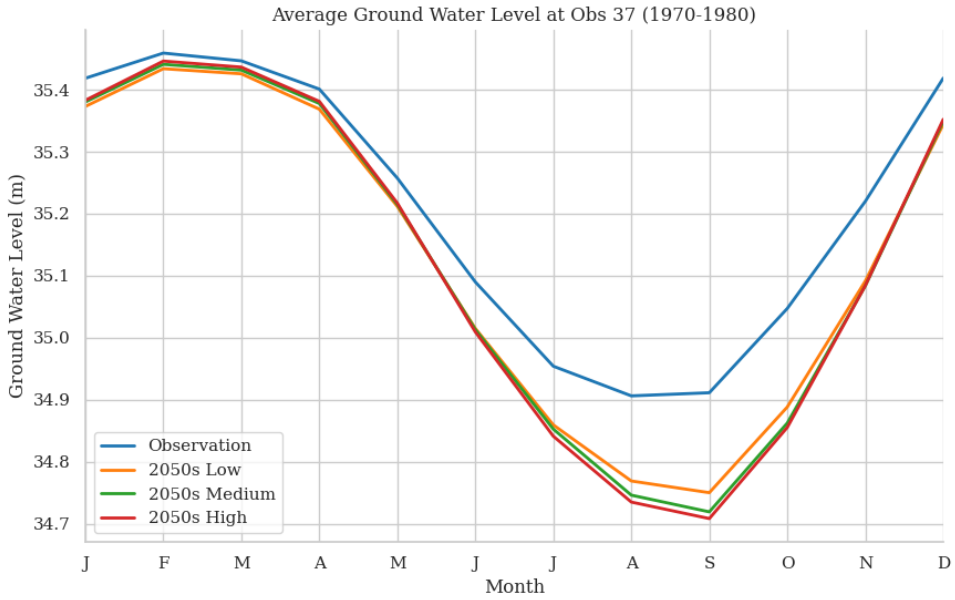

(e)Ground water level at Obs 37

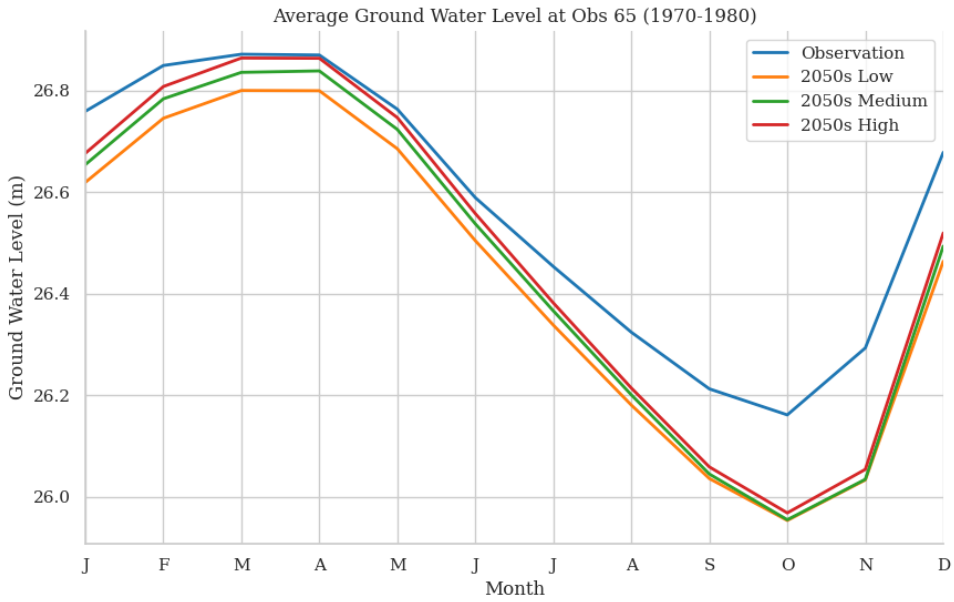

(f)Ground water level at Obs 65

Figure 9. The output results of model under 2050s scenarios (Low, Medium, High)

In these graphs, under the 2050s scenarios, both the ground water level and discharge in the model are lower than the reference observed values, particularly during periods with minimum values. Overall, the simulated group's trend remains consistent with the control group; however, the months with minimum values at Obs 35 and Obs 37 are delayed, from October to November and from August to September, respectively. Furthermore, except for Obs 37, where the simulation results among the high, medium, and low scenarios do not differ significantly, the values at other stations decrease in the order of high, medium, and low scenarios.

Discussion and conclusions

The results of this study provided significant insights into the performance of the MIKE-SHE distributed hydrological model. The calibration of the model revealed a high level of consistency between observed and simulated river discharge and groundwater levels (Henriksen *et al.*, 2003).

The catchment was more vulnerable to changes in potential evapotranspiration (PET) than precipitation, according to the climate change impact assessment. This result was in line with other research (Milly, Dunne and Vecchia, 2005), which underlined the significance of taking PET changes into account when evaluating the hydrological impacts of climate change.

Climate change was projected to impact precipitation patterns and potential evapotranspiration (PET) rates in the future. These changes would depend on the emissions scenario considered. The model findings demonstrated a drop in both

groundwater levels and river discharge for the three climate change scenarios (low, medium, and high emissions) compared to the reference observed values. The possible reason was that, under these scenarios, precipitation could become more unpredictable and intense (Trenberth, 2011). As a result, less water would be available to maintain river flows and recharge aquifers. This could result in a decrease in river discharge and groundwater storage, especially during dry periods when water is most limited (Roudier *et al.*, 2016). A rise in PET rates was also anticipated as a result of rising temperatures, an increase in solar radiation, and changes in atmospheric humidity. Water scarcity might be worse by increased PET rates because they could result in larger water losses through evaporation and plant transpiration (Fischer, Beyerle and Knutti, 2013).

These results emphasised the potential difficulties in managing water resources under climate change, as decreased groundwater levels and river discharge may have detrimental effects on water supply, ecosystem health, and the overall resilience of catchment systems. Understanding the link between climate change-induced changes in precipitation and PET, as well as their effects on groundwater levels and river flow, was critical for making effective adaptation measures and ensuring sustainable water resource management in a changing climate (Arnell, 2004).

References

Abbott, M.B. *et al.* (1986) ‘An introduction to the European Hydrological System — Systeme Hydrologique Europeen, “SHE”, 1: History and philosophy of a physically-based, distributed modelling system’, *Journal of Hydrology*, 87(1), pp. 45–59. Available at: https://doi.org/10.1016/0022-1694(86)90114-9.

Arnell, N.W. (2004) ‘Climate change and global water resources: SRES emissions and socio-economic scenarios’, *Global Environmental Change*, 14(1), pp. 31–52. Available at: https://doi.org/10.1016/j.gloenvcha.2003.10.006.

Bates, B. *et al.* (2008) *Climate Change and Water. Technical Paper of the Intergovernmental Panel on Climate Change*.

Brown, J.M., Souza, A.J. and Wolf, J. (2010) ‘An 11-year validation of wave-surge modelling in the Irish Sea, using a nested POLCOMS–WAM modelling system’, *Ocean Modelling*, 33(1), pp. 118–128. Available at: https://doi.org/10.1016/j.ocemod.2009.12.006.

Environment Agency, E.A. (2008) ‘Humber flood risk management strategy’. Available at: https://www.gov.uk/government/publications/humber-flood-risk-management-strategy.

Fischer, E.M., Beyerle, U. and Knutti, R. (2013) ‘Robust spatially aggregated projections of climate extremes’, *Nature Climate Change*, 3(12), pp. 1033–1038. Available at: https://doi.org/10.1038/nclimate2051.

Graham, D. and Butts, M. (2005) ‘Flexible, integrated watershed modelling with MIKE SHE’, in *Watershed Models*, pp. 245–272. Available at: https://doi.org/10.1201/9781420037432.ch10.

Henriksen, H.J. *et al.* (2003) ‘Methodology for construction, calibration and validation of a national hydrological model for Denmark’, *Journal of Hydrology*, 280(1), pp. 52–71. Available at: https://doi.org/10.1016/S0022-1694(03)00186-0.

Henriksen, H.J. *et al.* (2008) ‘Assessment of exploitable groundwater resources of Denmark by use of ensemble resource indicators and a numerical groundwater–surface water model’, *Journal of Hydrology*, 348(1), pp. 224–240. Available at: https://doi.org/10.1016/j.jhydrol.2007.09.056.

Hervouet, J.-M. (2007) ‘Hydrodynamics of Free Surface Flows: Modelling With the Finite Element Method’, *Hydrodynamics of Free Surface Flows: Modelling with the finite element method* [Preprint]. Available at: https://doi.org/10.1002/9780470319628.

Horsburgh, K.J. and Wilson, C. (2007) ‘Tide-surge interaction and its role in the distribution of surge residuals in the North Sea’, *Journal of Geophysical Research*, 112(C8), p. C08003. Available at: https://doi.org/10.1029/2006JC004033.

IPCC (2019) ‘Special Report on the Ocean and Cryosphere in a Changing Climate —’. Available at: https://www.ipcc.ch/srocc/ (Accessed: 27 April 2023).

Milly, P.C.D., Dunne, K.A. and Vecchia, A.V. (2005) 'Global pattern of trends in streamflow and water availability in a changing climate', *Nature*, 438(7066), pp. 347–350. Available at: https://doi.org/10.1038/nature04312.

National Research Council Canada (2019) *Blue Kenue™: software tool for hydraulic modellers*. Available at: https://nrc.canada.ca/en/research-development/products-services/software-applications/blue-kenuetm-software-tool-hydraulic-modellers (Accessed: 27 April 2023).

Needham, H.F., Keim, B.D. and Sathiaraj, D. (2015) 'A review of tropical cyclone-generated storm surges: Global data sources, observations, and impacts', *Reviews of Geophysics*, 53(2), pp. 545–591. Available at: https://doi.org/10.1002/2014RG000477.

Nicholls, R.J. *et al.* (2011) 'Sea-level rise and its possible impacts given a "beyond 4°C world" in the twenty-first century', *Philosophical Transactions. Series A, Mathematical, Physical, and Engineering Sciences*, 369(1934), pp. 161–181. Available at: https://doi.org/10.1098/rsta.2010.0291.

Pappenberger, F. *et al.* (2005) 'Uncertainty in the calibration of effective roughness parameters in HEC-RAS using inundation and downstream level observations', *Journal of Hydrology*, 302(1), pp. 46–69. Available at: https://doi.org/10.1016/j.jhydrol.2004.06.036.

Refsgaard, J.C. *et al.* (2013) 'The role of uncertainty in climate change adaptation strategies — A Danish water management example', *Mitigation and Adaptation Strategies for Global Change*, 18(3), pp. 337–359. Available at: https://doi.org/10.1007/s11027-012-9366-6.

Roudier, P. *et al.* (2016) 'Projections of future floods and hydrological droughts in Europe under a +2°C global warming', *Climatic Change*, 135(2), pp. 341–355. Available at: https://doi.org/10.1007/s10584-015-1570-4.

Thompson, J.R. *et al.* (2014) 'Climate change uncertainty in environmental flows for the Mekong River', *Hydrological Sciences Journal*, 59(3–4), pp. 935–954. Available at: https://doi.org/10.1080/02626667.2013.842074.

Trenberth, K. (2011) 'Changes in precipitation with climate change', *Climate Research*, 47(1), pp. 123–138. Available at: https://doi.org/10.3354/cr00953.

Wadey, M.P. *et al.* (2015) 'Assessment and comparison of extreme sea levels and waves during the 2013/14 storm season in two UK coastal regions', *Natural Hazards and Earth System Sciences*, 15(10), pp. 2209–2225. Available at: https://doi.org/10.5194/nhess-15-2209-2015.